

Article

A Novel 10-Parameter Motor Efficiency Model Based on I-SA and Its Comparative Application of Energy Utilization Efficiency in Different Driving Modes for Electric Tractor

Zhun Cheng ¹, Huadong Zhou ² and Zhixiong Lu ^{2,*}

¹ Department of Vehicle Engineering, College of Automobile and Traffic Engineering, Nanjing Forestry University, Nanjing 210037, China; chengzhun38@163.com

² College of Engineering, Nanjing Agricultural University, Nanjing 210031, China; lesprince_3@163.com

* Correspondence: luzx@njau.edu.cn

Abstract: To build a more accurate motor efficiency model with a strong generalization ability in order to evaluate and improve the efficiency characteristics of electric vehicles, this paper researches motor efficiency modeling based on the bench tests of two motor efficiencies with differently rated powers. This paper compares and analyzes three motor efficiency modeling methods and finds that, when the measured values in motor efficiency tests are insufficient, the bilinear interpolation method and radial basis kernel function neural networks have poor generalization abilities in full working conditions, and the precision of polynomial regression is limited. On this basis, this paper proposes a new modeling method combining correlation analysis, polynomial regression, and an improved simulated annealing (I-SA) algorithm. Using the mean and the standard deviation of the mean absolute percentage error of the 5-fold Cross Validation (CV) of 100 random tests as the evaluation indices of the precision of the motor efficiency model, and based on the motor efficiency models with verified precision, this paper makes a comparative analysis on the full vehicle efficiency of electric tractors of three types of drive in five working conditions. Research results show that the proposed novel method has a high modeling precision of motor efficiency; tractors with a dual motor coupling drive system have optimal economic performance.

Keywords: electric tractor; motor efficiency; dual motor coupling drive; I-SA algorithm; generalization ability; parameter identification



Citation: Cheng, Z.; Zhou, H.; Lu, Z. A Novel 10-Parameter Motor Efficiency Model Based on I-SA and Its Comparative Application of Energy Utilization Efficiency in Different Driving Modes for Electric Tractor. *Agriculture* **2022**, *12*, 362. <https://doi.org/10.3390/agriculture12030362>

Academic Editors: Mustafa Ucgul and Chung-Liang Chang

Received: 28 January 2022

Accepted: 28 February 2022

Published: 3 March 2022

Publisher's Note: MDPI stays neutral with regard to jurisdictional claims in published maps and institutional affiliations.



Copyright: © 2022 by the authors. Licensee MDPI, Basel, Switzerland. This article is an open access article distributed under the terms and conditions of the Creative Commons Attribution (CC BY) license (<https://creativecommons.org/licenses/by/4.0/>).

1. Introduction

Electric vehicles use a motor as the core power source [1,2] and electric energy as the driving energy [3]. This is not only convenient for recycling energy, but it can also achieve low emissions or even zero emissions [4–6]. In addition, electric energy can be obtained widely and conveniently. Compared with internal combustion engine vehicles, electric vehicles also have the advantages of low noise and low maintenance costs [7]. These characteristics provide great help for the sustainability of the environment and its ecology. A purely electric vehicle can realize zero release, and its energy is widely and easily available. Currently, for all types of vehicles, researchers are continuously studying and developing drive systems with the motor as the power supply unit, including those in vehicles such as the electric truck [8], the refuse collection truck [9], the electric urban delivery truck [10], the electric car [11–14], electric agricultural machinery [15], etc. Especially in the research field of agricultural machinery, agricultural machinery faces complicated working conditions. Agricultural machinery such as tractors generally needs to meet the requirements of operation, including ploughing, rotary tillage, transportation, and normal road driving [16,17]. Therefore, the research and application of electric tractors can help to overcome the problems of the traditional tractor, such as complicated variable transmission structures, frequent operation of the driver, limited energy utilization efficiency, etc. [18–20].

At the current stage, the multi-power-source purely electric vehicle has certain advantages in price, energy consumption, power transmission, system efficiency, etc., compared with the single-motor drive vehicle and the hybrid-power vehicle [21]. The two main types of purely electric vehicles are as follows: distributed independent drive and centralized coupling drive. In addition, there are few studies on electrical agricultural machinery. Zhou et al. [22] proposed a wheel-rim motor independent drive scheme, aiming to give the four-wheel drive electric tractor better tractive performance in the working condition of traction operation. Han et al. [23] made a simulated analysis on the steering characteristics of wheel-rim drive electric tractors in heavy-load low-speed working conditions and in light-load high-speed working conditions. Xie et al. [24] proposed an overall structure scheme of dual-wheel drive electric tractors (the two rear driving wheels are driven by the motor independently) and tested the tractive performance, loaded starting and transportation working condition through the bench test. Li et al. [25] designed, compared and analyzed many dual-motor power coupling structure schemes based on the planetary gear train. The research built a dual-motor power coupling unit transmission simulation model using the software Simulation X.

Besides the type of energy used, energy consumption and emission control are also affected by system transmission efficiency. Using the electric tractor as an example, the efficiency characteristics of a power transmission system with the core of a motor plays a decisive role in the full vehicle's economic performance and in its energy utilization performance. Therefore, the correct description and modeling of efficiency characteristics of motors have great significance and necessity. However, currently there are few studies on the modeling of motor efficiency characteristics. Most researchers used polynomial regression, the bilinear interpolation method, and the table look-up method to build efficiency models, and they made subsequent research and applications based on the models. Additionally, most studies on electric vehicles' kinetic analysis, control, and performance improvements require considering motor efficiency. Ma et al. [26] proposed a planetary gear coupling mechanism based on the dual motor structure and used the particle swarm optimization method to optimize the parameters of the transmission system. Their research was made according to the efficiency characteristics of motors. Hu et al. [27] proposed a new dual motor coupling power drive system and combined the efficiency characteristics of motors to analyze and make power distribution strategies for different drive modes. Li et al. [28] used a motor efficiency model for parameter matching, power management strategy development, and power distribution control research of a dual motor coupling drive system. Their research measured and recorded the data of torque, speed, and efficiency through a bench test and then obtained the motor efficiency in any state using the interpolation method. Li et al. [29] designed a dual motor multi-mode power coupling drive system for the purely electric tractor (the system can realize four drive modes) and made a simulation test on the ploughing and transportation working conditions of tractors. Their research used the quasi-static maps of output speed and torque to build the dual motor efficiency model and to obtain the motor efficiency in any working state though the table look-up method. Chen et al. [30] pointed out that the current studies on power system parameter design focused mainly on electric cars but less on electrical agricultural machinery. Their research used a quantified motor efficiency to optimize the system in order to improve the performance of electric tractors.

Therefore, for electric vehicles, the evaluation, analysis, and improvement on their power performances and economic performances should be made according to the efficiency characteristics of motors. In addition, the design of reasonable and effective power transmission systems and parameter matches also depend on the efficiency characteristics of motors. Therefore, building an accurate model of motor efficiency characteristics is an important premise of the design, control, and improvement of electric vehicles. However, different motors have different efficiency characteristics and change laws. Therefore, only the modeling of motor efficiency characteristics with specific test data and scientific verification methods is effective. In addition, building a motor efficiency model with a

specific mathematical expression form can further help the kinetic analysis and control of the system. In addition, current studies on electric vehicles such as the electric tractor focus mainly on the comparison of an electrically driven car and a railway motor car and on the comparison of a single motor and multiple motors, but there are few comparative studies on the working efficiency of dual motor coupling drives, of dual motor rear wheel independent drives, and of four-wheel independent drives based on the wheel hub motor.

Based on the above literature, there are some deficiencies in the research of electric vehicles at the present stage: (1) There is more research on electric vehicles but less research on electric agricultural machinery. (2) Comparative studies on distributed independent drives and on centralized coupling drives of tractors with multiple power sources are relatively less abundant. This makes it difficult to develop a drive system with relatively better performance in the conceptual design stage, although the actual characteristics of the motor have been obtained. (3) There are many research papers on the application of motor efficiency but few studies on the establishment of the motor efficiency characteristics model. (4) Polynomial regression, bilinear interpolation, and the table look-up method are often used to establish the motor efficiency characteristics model, which lacks the application and comparison of advanced modeling methods, resulting in limited precision of model estimation. (5) The interpolation method and the table look-up method are difficult to use to form specific mathematical expressions, so the effect of extrapolation prediction is limited. (6) When polynomial regression is applied, only the power function form of speed and torque and the interaction term of each order are considered, and the influence of other data transformation forms on the efficiency characteristics of the motor is not explored.

In order to solve the above problems, combined with the bench test data of tractor motors, this paper aims to put forward a model to correctly describe the efficiency characteristics of motors by comparing four different modeling methods and by exploring the influence of other data transformation forms of physical quantities (speed and torque) on the efficiency characteristics of motors. In addition, the efficiency of tractors' different driving systems is compared and analyzed through the measured data and the new model (based on the typical multiple working conditions of tractors). This provides a direct basis for the further research and development of electric tractor drive systems and for the establishment of a high precision motor model. Specifically, this paper proposes a 10-parameter motor efficiency modeling method combining the correlation coefficient and the improved simulated annealing (I-SA) algorithm. The method mainly adopts the idea of polynomial regression and error compensation. According to the measured data of motor efficiency through the bench test, an initial fitting model made through polynomial regression analysis is built. In the case of the lack of polynomial regression precision, the variable with the maximum correlation is determined according to the calculation of the correlation coefficient, and it is introduced into the initial fitting model as a compensation variable to obtain a new motor efficiency model. Additionally, the proposed method identifies the parameters of a new model of motor efficiency using the I-SA algorithm according to the bench test data. Then, the new model of motor efficiency is built. To improve and verify the effectiveness and precision of the new efficiency model, this paper uses the mean of the 5-fold Cross Validation (CV) accuracy of multiple tests as the evaluation index and comparatively analyzes the novel modeling method with those using polynomial regression (PR), the bilinear interpolation method (BI), and the radial basis kernel function neural network (RBF-NN). This paper uses two motors with different powers of tractors in the research. Finally, this paper researches and comparatively analyzes the differences among three drive types (the dual motor coupling drive, the dual motor rear wheel independent drive, and the four-wheel independent drive based on wheel hub motor) of multi-power-source purely electric vehicles in working efficiency with their motor efficiency models built. This paper uses different reserve power states of electric tractors, including the running speed working condition, the normal running working condition, the transportation working condition, the ploughing working condition, and the rotary tillage working condition, as examples for the comparison of the efficiency characteristics of full vehicles.

2. Materials and Methods

2.1. Characteristic Analysis of the Distributed Independent Drive System

Figure 1 gives a structural diagram of a dual motor dual-wheel distributed independent drive system [31]. (The drive system is mainly composed of two independent motors and two independent reducers. The left rear wheel or right rear wheel is driven by a separate “wheel side motor-reducer” system.) Figure 2 gives a structural diagram of a four-motor four-wheel distributed independent drive system [22,32]. (Approximate to the dual motor dual-wheel distributed drive system, four wheels of the vehicle are driven by four separate “wheel motor-reducer” systems.) Different from the traditional “combustion-motor-variable-transmission-unit” and the single-motor-variable-transmission-unit structural forms, the distributed independent drive system removes most mechanical connection mechanisms (mainly referring to complicated mechanical transmission mechanisms such as the gearbox, the differential mechanism, etc.). Using a tractor as an example, the drive system increases the flexibility of the spatial structure arrangement greatly and helps realize the light weight of a full vehicle.

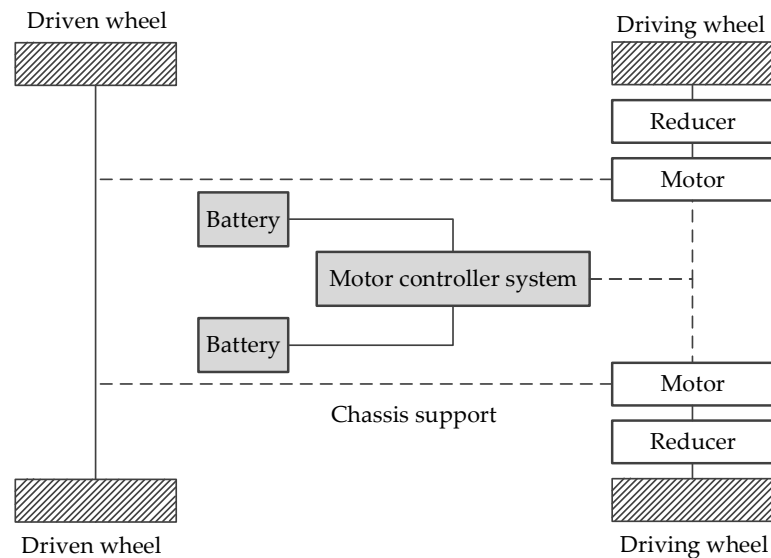


Figure 1. Structural diagram of dual motor dual-wheel distributed independent drive system.

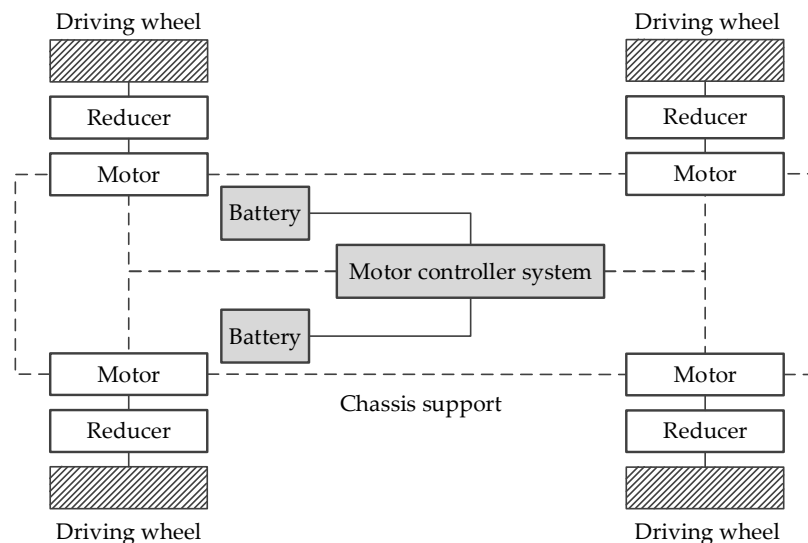


Figure 2. Structural diagram of four-motor four-wheel distributed independent drive system.

According to Figures 1 and 2, the calculation formula of speed-regulating characteristics of a distributed independent drive system is as follows:

$$u_a = 3.6 \times 2\pi(n_m r_d) / (60i_g) \tag{1}$$

where u_a is the running speed of the electric vehicle (km/h), r_d is the rolling radius of the driving wheel (m), i_g is the transmission ratio of the reducer, and n_m is the output speed of the motor (r/min).

The following is the calculation formula of the torque of the distributed independent drive system:

$$nT_m i_g / r_d = F_L \tag{2}$$

where n is the number of the motor of the distributed independent drive system, T_m is the output torque of a single motor (Nm), and F_L is the carrying capacity of the electric vehicle (N).

The following is the calculation formula of efficiency characteristics of the distributed independent drive system:

$$\eta_{sys1} = \eta_m(n_m, T_m)\eta_0 \tag{3}$$

where η_{sys1} is the efficiency value of the distributed independent drive system, η_m is the efficiency of the motor (a function with motor speed n_m and torque T_m as independent variables), and η_0 is the overall working efficiency of other systems (mainly composed of the efficiency of the storage battery, the efficiency of the reducer, etc.) and is also a fixed value in this paper.

2.2. Characteristic Analysis of a Dual Motor Centralized Coupling Drive System

Figure 3 gives a structural diagram of a dual motor centralized coupling drive system used in this paper [33]. The system is a speed coupling drive system. The power output from motor 1 and motor 2 is transmitted into the planetary gear train’s gear ring and sun gear. The two parts of power converge through the planetary gear structure and then are output through the planetary carrier. The power output passes through the reducer and the differential mechanism and then forms the power of the driving wheels.

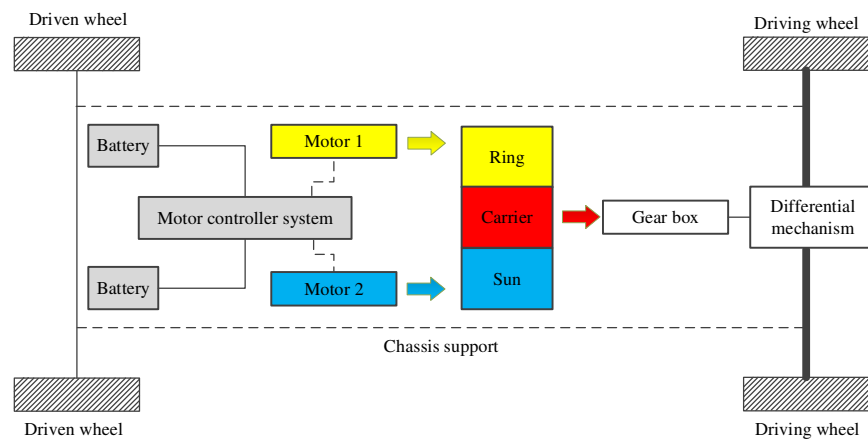


Figure 3. Structural diagram of dual motor centralized coupling drive system.

The following is the calculation formula of the speed-regulating characteristics of the dual motor centralized coupling drive system:

$$u_a = 0.377 \frac{k_p n_{m1} + n_{m2}}{(1 + k_p) i_g} r_d \tag{4}$$

where k_p is the characteristic parameter of the planetary row and n_{m1} and n_{m2} (r/min) are the output speeds of motor 1 and motor 2, respectively.

The following is the calculation formula of the torque of the dual motor centralized coupling drive system:

$$\frac{T_{m1}}{k_p} = T_{m2} = \frac{F_L r_d}{i_g} \tag{5}$$

where T_{m1} and T_{m2} (Nm) are the output torques of motor 1 and motor 2, respectively.

This paper analyzes the loss of power flow in motor 1, motor 2, and the planetary gear train to deduce the overall efficiency characteristics of the system. By dividing the whole system into a series subsystem (mainly motor 1 to the gear ring; motor 2 to the sun wheel; planetary carrier to the other transmission systems) and a parallel subsystem (mainly confluence mechanisms), the efficiency characteristics model is then obtained by combining the series and parallel subsystems [16,34].

The calculation formula of the efficiency characteristics of the dual motor centralized coupling drive system is as follows:

$$\eta_{sys2} = k_p (\eta_{rc} \eta_{m1} n_{m1} + \eta_{sc} \eta_{m2} n_{m2} / k_p) / (k_p n_{m1} + n_{m2}) \eta_0 \tag{6}$$

where η_{sys2} is the efficiency of the dual motor centralized coupling drive system, η_{rc} is the transmission efficiency of the power flow from the gear ring to the planetary carrier, and η_{sc} is the transmission efficiency of power flow from the sun gear to the planetary carrier.

This paper uses the transmission ratio method [16,35] to calculate the transmission efficiency η_{rc} of power flow from the gear ring to the planetary carrier and the transmission efficiency η_{sc} of the power flow from the sun gear to the planetary carrier. The calculation formula is as follows:

$$\eta_{sc} = \frac{1 + k_p \eta_c \text{sign}[\frac{k_p}{1+k_p} \times \frac{\partial(1+k_p)}{\partial(k_p)}]}{1 + k_p} \tag{7}$$

$$\eta_{rc} = \frac{1 + k_p \eta_c \text{sign}[\frac{k_p^2}{1+k_p} \times \frac{\partial(\frac{1+k_p}{k_p})}{\partial(k_p)}]}{\eta_c \text{sign}[\frac{k_p^2}{1+k_p} \times \frac{\partial(\frac{1+k_p}{k_p})}{\partial(k_p)}] (1 + k_p)} \tag{8}$$

where η_c is the friction transmission efficiency of the 2K-H planetary gear train.

2.3. Obtaining the Measured Data of the Bench Test of Motor Efficiency

This paper uses two motors of electric tractors as examples to obtain related data of the motors through the bench test. The two motors are both brushless direct current motors. Table 1 shows the specific parameters.

Table 1. Related parameters of the motor.

Type	Rated Power/kW	Rated Speed/r/min	Rated Torque/Nm
Brushless DC motor	5	750	63
Brushless DC motor	8	850	90

The test bench uses a lithium battery pack with a total voltage of 211.2 V to offer power (see Table 2 for the main parameters of the power battery) and a magnetic powder brake as the simulation loading unit (Table 3 shows the parameters of the magnetic powder brake). The information of the overall layout of the test bench, the design of the observation and control plan, the equipment installation and debugging, and the calibration of the sensors (mainly including the current sensor, the voltage sensor and the speed torque sensor) can be found in previous studies [22,36].

Table 2. Related parameters of power battery.

Type	Nominal Voltage of Monomer/V	Number of Monomers	Nominal Capacity of Monomer/(A·h)	Total Voltage/V
Lithium battery	3.3	64	100	211.2

Table 3. Related parameters of magnetic powder brake.

Model	Rated Torque/Nm	Magnetizing Current/A	Allowable Slip Power/kW	Cooling Mode
CZ-20	200	2	10	Water cooling

Figure 4 shows the test bench of the motor.

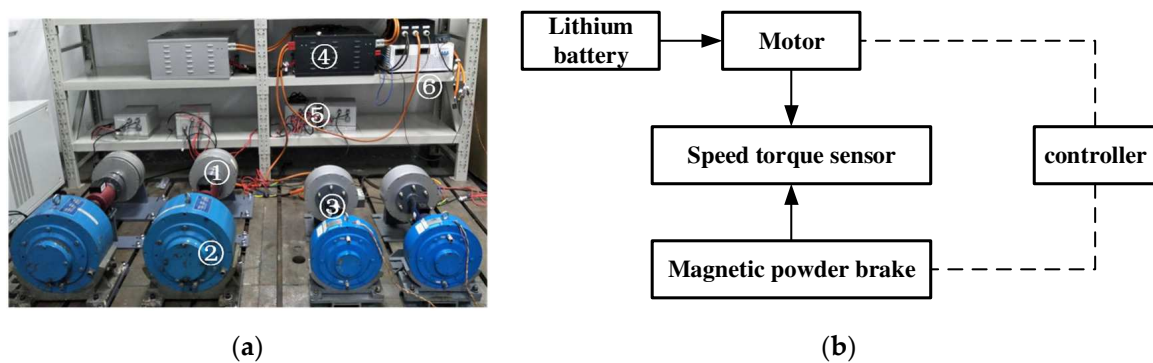


Figure 4. Structural composition of motor test bench. Note: ① Motor used in the research; ② magnetic powder brake; ③ speed torque sensor; ④ lithium battery; ⑤ motor controller; ⑥ power management system. (a) The picture of test site; (b) Schematic diagram.

The detailed steps of the motor efficiency test can be found in previous studies [22,36]. For the test, load the motor through the magnetic powder brake. Each loading should be performed after the motor’s working speed remains stable. The efficiency test results of the 8 kW motor came from a reference document [36]. The following is the calculation formula of the motor efficiency:

$$\eta_m = \frac{P_{out}}{P_{in}} = \frac{T_m n_m}{9.55UI} \tag{9}$$

where P_{out} is the mechanical power output of the motor (W), P_{in} is the input power of the motor (W), U is the input voltage of the motor (V), and I is the current input of the motor (A).

Figure 5 shows the measured results of efficiency of two motors used in the analysis.

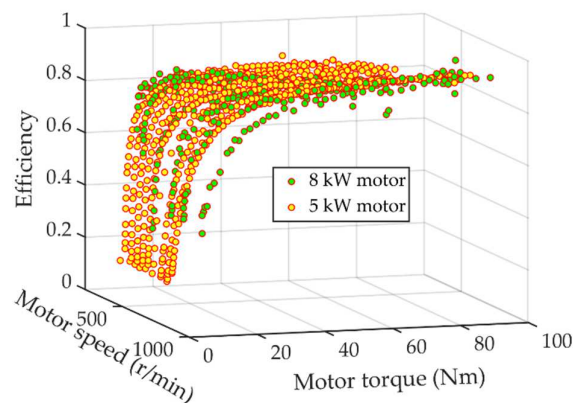


Figure 5. Measured results of efficiency of two motors.

2.4. Three Modeling Methods of Motor Efficiency

Current studies generally use PR [37] and BI as the modeling methods of motor efficiency. Therefore, to comparatively analyze the differences among the modeling methods of motor efficiency comprehensively, this paper also uses PR and BI as the modeling methods for the comparative analysis. Additionally, this paper chooses the neural network as one of modeling methods for comparative analysis. This paper uses the RBF-NN.

The PR model considers the 1-order term, the 2-order term, and the interaction term of the motor speed n_m and the motor torque T_m , and its expression is as follows:

$$\eta_{m_PR} = a_0 + a_1n_m + a_2T_m + a_3n_mT_m + a_4n_m^2 + a_5T_m^2 \tag{10}$$

where η_{m_PR} is the motor efficiency model built using PR and $a_0 \sim a_5$ are the coefficients of the order terms of the polynomial.

The BI method [38] requires the information of four data points and makes the linear interpolation in two directions of coordinate axes to finally determine the data value of the points to be interpolated.

The RBF-NN was proposed by J. Moody and C. Darken in 1989, and it is a forward local neural network that can approach any nonlinear function with any arbitrary small error [39–41]. Currently, the RBF-NN has a wide range of applications, and many scholars have found in studies that the RBF-NN is superior to the conventional BP neural network in every respect. Figure 6 shows the topological structure of the RBF-NN.

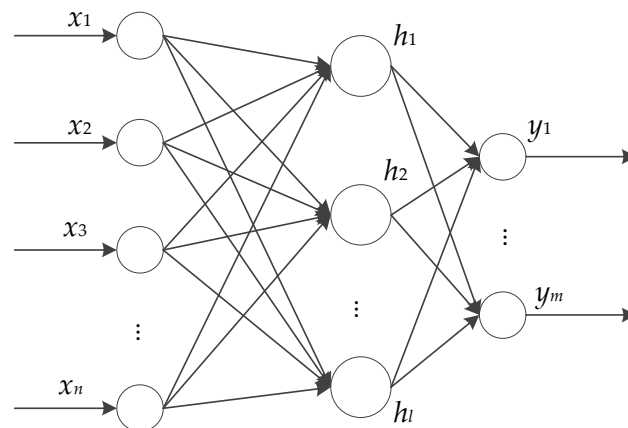


Figure 6. Technical route of establishing dynamic load characteristics prediction model. Note: $x = [x_1, x_2, \dots, x_n]$ represents the input vector; $h = [h_1, h_2, \dots, h_l]$ represents the middle layer; $y = [y_1, y_2, \dots, y_m]$ represents output vector.

In Figure 6, $x = [x_1, x_2, \dots, x_n]$ represents the input vector. The middle layer uses a Gauss function for the nonlinear transformation of the input vector to obtain $h = [h_1, h_2, \dots, h_l]$ and then a linear weighting combination to obtain $y = [y_1, y_2, \dots, y_m]$ and considers it as the output. The calculation formula is as follows:

$$y_i = \sum_{j=1}^l w_{ij}h_j = \sum_{j=1}^l [w_{ij} \exp\{-\frac{(x - c_j)^T(x - c_j)}{\delta_j^2}\}] \tag{11}$$

where $i = 1, \dots, m$, of which m is the dimension of the output, l is the number of neurons in the hidden layer, and w_{ij} is the connection weight of the i output and the j neuron in the hidden layer.

To build an efficiency model based on the RBF-NN more comprehensively, this paper uses PR's idea of 1-order terms and 2-order terms using the motor speed n_m and the motor torque T_m , and it also uses interaction term modeling, which considers the 1-order term,

the 2-order term, and the interaction term of the motor speed n_m and the motor torque T_m as the characteristic variables of neural network learning and training.

Additionally, to further compare the modeling methods of motor efficiency comprehensively, this paper uses the 5-fold CV method [42]. This paper uses the mean and standard deviation of the MAPE (mean absolute percentage error) of the 5-fold CV of 100 random tests as the indices to evaluate the precision of the motor efficiency model.

The following is the calculation formula of the MAPE:

$$MAPE = \frac{1}{n} \sum_{i=1}^n \left| \frac{\eta_{m_estimated} - \eta_{m_measured}}{\eta_{m_measured}} \right| \times 100\% \quad (12)$$

where $\eta_{m_estimated}$ is the evaluated value based on the motor efficiency model, $\eta_{m_measured}$ is the measured value of motor efficiency, and n is the total number of data of the training set or the test set.

2.5. A Novel 10-Parameter Modeling Method of Motor Efficiency Using the I-SA for Parameter Identification

Although BI and the RBF-NN can build the motor efficiency model effectively (see Section 3.1), the models built with the two methods (have passed the 5-fold CV, see Section 3.1) have ideal and high precision for both the learning and training samples and the test samples. However, according to research results in this paper (Section 3.1), the precision of the motor efficiency models built with BI and RBF-NN depends on the value range of the learning and training sample data (i.e., the value range of motor speed n_m and motor torque T_m in the learning and training samples). If the set of test data is in the value range of motor speed n_m and motor torque T_m in the learning and training samples, the two methods can offer the estimated value of motor efficiency with high precision. If the set of test data is out of the value range of the motor speed n_m and the motor torque T_m in the learning and training samples, BI cannot be implemented due to the limitations of required conditions. Additionally, the RBF-NN's extrapolation prediction result is poor.

In addition, BI and the RBF-NN have no directly simple relational expression, so they are rather complicated and tedious in practical applications.

To sum it up, the two methods are limited in their generalization abilities and are applicable to the case with a mass of bench test data. Therefore, the two methods are inapplicable to the technical research and development of real-time adjustment full vehicle control strategies according to the current efficiency of intelligent vehicle systems.

However, PR has limited precision (see Section 3.1). According to the problems above, this paper proposes a modeling method of motor efficiency, combining the correlation coefficient and PR. Using the idea of error compensation for reference and considering the limited precision of PR, the method uses the enumeration method and correlation coefficient analysis to determine the variable with the maximum correlation, it introduces the variable into the PR model as a compensation term, and it finally forms a new model. In addition, the motor torque T_m 's correlation with efficiency is bigger than that of the motor speed. with efficiency, so the 3-order term of the motor torque T_m is introduced into the new model. The new model's expression is as follows:

$$\eta_{m_novel} = a_0 + a_1 n_m + a_2 T_m + a_3 n_m T_m + a_4 n_m^2 + a_5 T_m^2 + a_6 T_m^3 + a_7 f(a_8 x + a_9) \quad (13)$$

where η_{m_novel} is the novel 10-parameter model of motor efficiency, $a_0 \sim a_9$ are the coefficients of the order terms of the polynomial, $f(x)$ is the mapping function with x as the independent variable, and x is the motor speed n_m or the motor torque T_m .

The novel model has high nonlinearity. This paper uses the I-SA algorithm and combines the bench test data for the parameter identification of the novel model of motor efficiency and then completes the building of the novel model of motor efficiency.

As a result of the sample data involved in this case being large, the optimization process is nonlinear in the pursuit of high modeling precision. The heuristic intelligent

optimization algorithm [43–45] is suitable for solving a series of complex engineering problems accurately. This paper adopts the SA algorithm as the method of parameter identification. The SA algorithm used in this paper refers to the flow of the I-SA algorithm that has been proposed and that verified the engineering application effect in previous studies [46,47]. The applied I-SA algorithm is mainly improved in the following aspects: (1) termination conditions of algorithm iteration; (2) disturbance function; and (3) the updating method of decision variables. The specific algorithm flow is shown in Figure 7. This paper considers the mean of the MAPE of the 5-fold CV as the objective function of the I-SA algorithm.

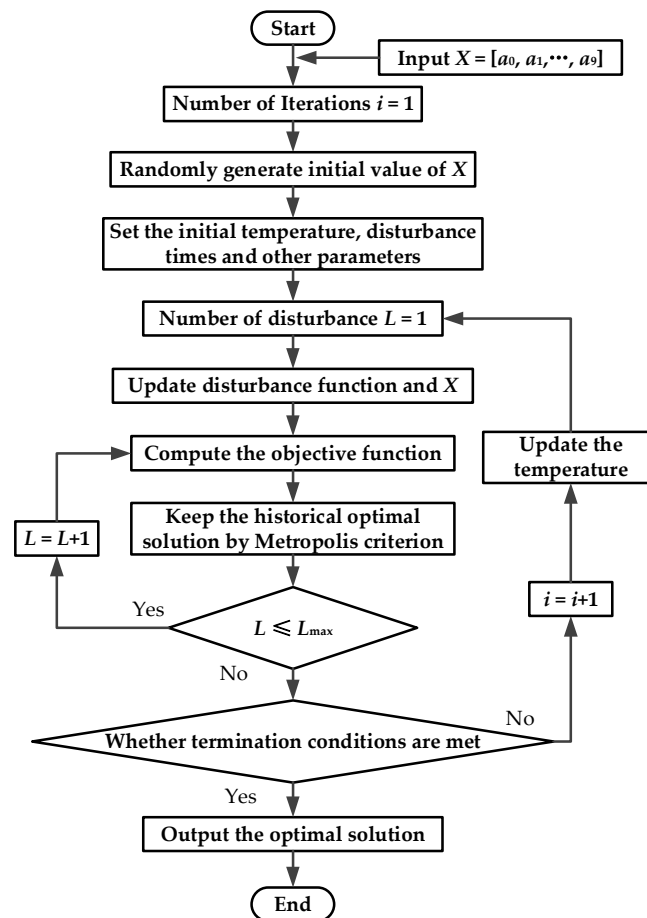


Figure 7. Flow diagram of the I-SA algorithm. Note: L is number of disturbances; X is the set of decision variables; i is number of Iterations; L_{\max} is maximum number of disturbances.

In this paper, the I-SA algorithm is used to complete the parameter identification of the new model with ten parameters to finally complete the establishment of the motor efficiency characteristics model. Figure 8 shows the building process of the novel model of motor efficiency.

2.6. Comparative Analysis Method of the Full Vehicle Efficiency Characteristics of Electric Tractors in Five Working Conditions

This paper applies the motor efficiency model to the comparative analysis of the work efficiency of multi-power-source electric vehicles of three drive types (i.e., the dual motor coupling drive, the dual motor rear wheel independent drive, and the four-wheel independent drive based on hub motor). This paper uses the electric tractor as an example. See Table 4 for the related parameters of the full vehicle.

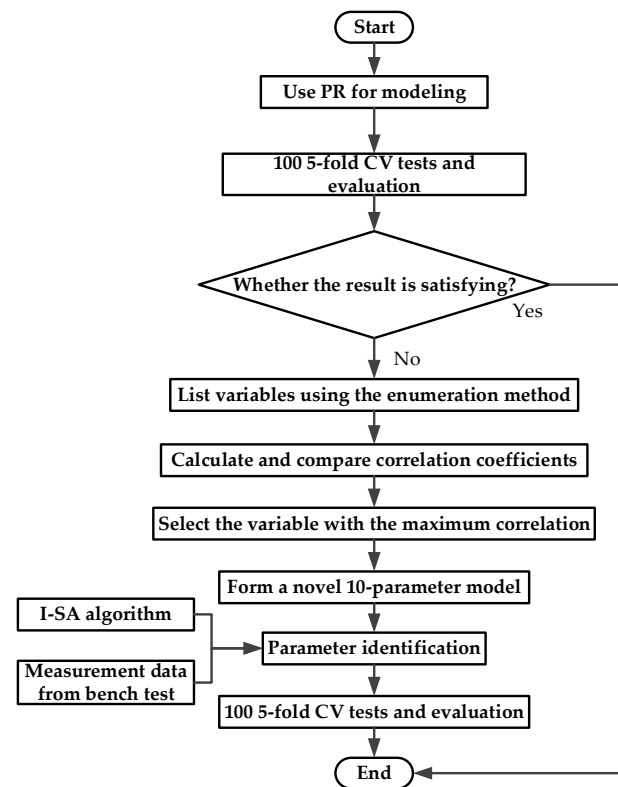


Figure 8. Flow diagram of building method of motor efficiency. Note: PR is Polynomial Regression; CV is Cross Validation; I-SA algorithm is Improved-Simulated Annealing algorithm.

Table 4. Related parameters of electric tractor.

Total Weight/kg	Radius of Driving Wheel/m	Coefficient of Air Resistance	Windward Area/m ²	Maximum Trailer Weight/kg
1535	0.64	0.9	3.135	1000

As for the running speed working condition of the electric tractor, this paper uses scholar Wang’s analysis on the research results of Resch and Renius for reference [48]. The results show that, in the overall life cycle, the tractor spends 61–68% of its time working in the speed range of 4–12 km/h.

This paper considers the average full vehicle efficiency of full working ranges in five working conditions of electric tractors as the evaluation index, and it uses it to compare the working efficiency of three drive types. The five working conditions are as follows:

(1) The electric tractors have different reserve power (the residual power eliminating the basic running resistance) and running speeds. The working condition is a general working condition for analysis, used to analyze the full vehicle working efficiency of electric tractors with different loads and running speeds.

The calculation formula of the reserve power is as follows:

$$F_{RF} = \frac{T_{out}}{r_d} - F_f - F_w = \frac{T_{out}}{r_d} - m_1 g f - \frac{C_D A u_a^2}{21.15} \tag{14}$$

where F_{RF} is the reserve power (N), T_{out} is the torque of the system power output to the driving wheel (Nm), F_f is the rolling resistance (N), F_w is the air resistance (N), m_1 is the overall weight of the electric tractor (kg), f is the rolling resistance coefficient, g is the acceleration of gravity, C_D is the coefficient of air resistance, and A is the windward area (m²).

(2) The electric tractor is in the normal road running condition with a constant speed. In this working condition, the drive system composed of the motor only needs to overcome the basic running resistance.

(3) The electric tractor is in the transportation working condition with a running speed of 12 km/h. The calculation formula of the loading force in the current working condition is as follows:

$$F_{TC} = (m_1 + m_2)gf + \frac{C_D A u_a^2}{21.15} \quad (15)$$

where F_{TC} is the loading force in the transportation working condition (N) and m_2 is the mass of the trailer of the electric tractor (kg).

(4) The electric tractor is in the ploughing working condition with a running speed of 10 km/h. The calculation formula of the loading force in the current working condition is as follows:

$$F_{PC} = F_f + F_w + kn_1bH \quad (16)$$

where F_{PC} is the loading force in the ploughing working condition (N), k is the soil-specific resistance, b is the width of a single plough, n_1 is the number of the plough share, and H is the tillage depth.

(5) The electric tractor is in the rotary tillage working condition with a running speed of 5 km/h. The calculation formula of the loading force in the current working condition is as follows:

$$F_{RTC} = F_f + F_w + k_2k_\lambda B_n h \quad (17)$$

where F_{RTC} is the loading force in the rotary tillage working condition (N), k_2 is the rotary tillage resistance calculation coefficient, k_λ is the soil-specific resistance of the rotary tillage, B_n is the tillage width, and h is the tillage depth.

Specifically, the multi-power-source purely electric tractors of three drive types include the 4 wheel independent drive electric tractor composed of four 5 kW motors, the rear wheel independent drive electric tractor composed of two 8 kW motors, and the coupling drive electric tractor composed of two 8 kW motors.

3. Results and Discussion

3.1. Modeling Results of Motor Efficiency Based on PR, BI, and the RBF-NN and Analysis

This paper uses the 5 kW motor of the electric tractor in Section 2.3 as an example, and there are a total of 510 measured data samples of the bench.

This paper uses the 5-fold CV method of 100 random tests. Figures 9 and 10, and Table 5 show the modeling results of the motor efficiency based on PR, BI, and the RBF-NN.

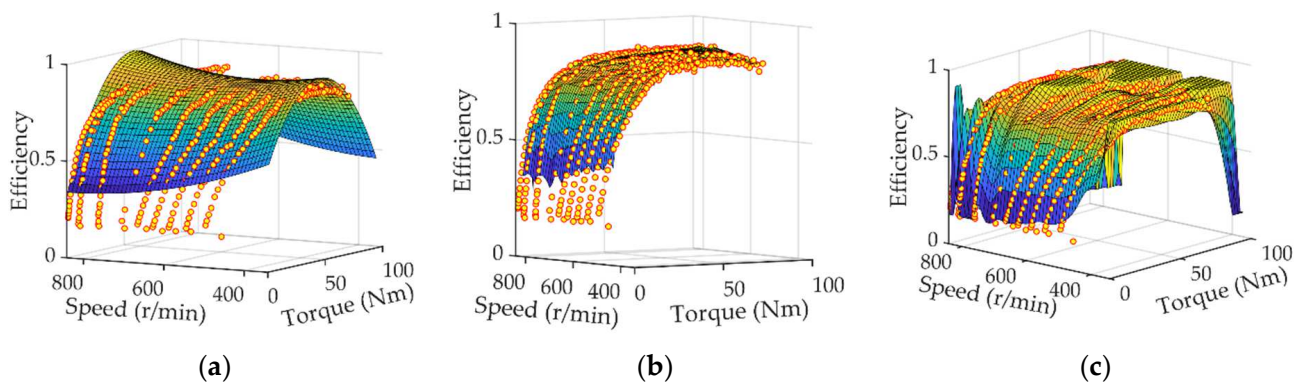


Figure 9. The comparison of precision of motor efficiency models in full working conditions. (a) Polynomial Regression; (b) Bilinear Interpolation method; (c) Radial Basis Kernel Function Neural Network.

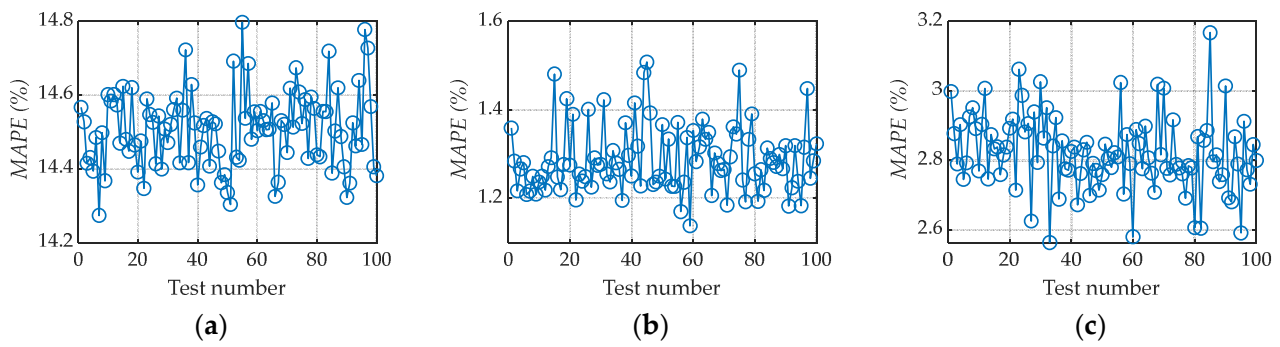


Figure 10. Comparison of results of 100 5-fold CV tests. (a) Polynomial Regression; (b) Bilinear Interpolation method; (c) Radial Basis Kernel Function Neural Network.

Table 5. Results of 5-fold CV of 100 random tests of four methods.

	PR	BI	RBF-NN	Novel Method Proposed
Mean (%)	14.51	1.29	2.84	2.45
Standard Deviation (%)	0.11	0.08	0.14	0.12

According to Figures 9 and 10 and Table 5, BI has the highest modeling precision followed by the RBF-NN, whereas PR has a certain difference compared with the other two methods. The results of the 5-fold CV of 100 random tests (of which the standard deviation is generally small) show that the three modeling methods of motor efficiency all have high reliability.

However, according to the research process in this paper, when using BI, there are invalid data points of motor efficiency generated in the test data set as a result of BI, which is limited by required calculation conditions, not being able to predict the working conditions out of the range of the learning and training set. This paper adds together the number of invalid data points in the 100 5-fold CV tests, and the results are shown in Figure 11.

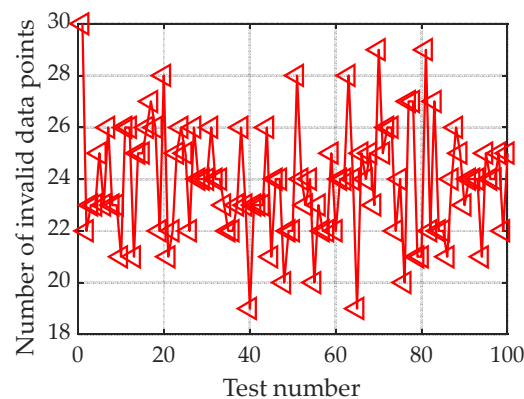


Figure 11. Statistical results of the number of invalid data points.

According to Figure 11, when using BI, if the number of measured data samples of motor efficiency is insufficient, there is an interpolation invalidation phenomenon. According to the results of the 100 5-fold CV tests, each model can generate about 24 invalid data points on average. Additionally, if the number of measured data samples of motor efficiency is insufficient, the estimation precision of BI for the nonlinear change section can decrease significantly.

According to Figures 9 and 10, and Table 5, although using the RBF-NN can estimate motor efficiency with high precision, the estimation precision for the change sections of

the motor speed n_m and the motor torque T_m out of the change range of the learning and training set decreases significantly.

To sum it up, BI and the RBF-NN depend on learning and training samples greatly. When the change ranges of the motor speed n_m and the motor torque T_m in the learning and training samples cover the whole domain of definition, BI and the RBF-NN have high motor efficiency estimation and modeling precision. Therefore, for the modeling of motor efficiency, BI and the RBF-NN have weak generalization abilities. In addition, neither BI nor the RBF-NN has a directly easy relational expression, causing complicated and tedious applications in practice (compared with PR). In addition, the requirement of many learning and training data for effective modeling also causes the two methods to be inapplicable to the research and development of adaptively adjusting motor efficiency MAP charts for real-time correcting control strategies of intelligent vehicle systems.

The advantages and disadvantages of the three modeling methods are summarized in Table 6.

Table 6. Comparison of advantages and disadvantages of three modeling methods.

Methods	Advantages	Disadvantages
Polynomial regression	Small standard deviation, high reliability of the model; fewer model parameters and less dependence on the number of data; clear and simple mathematical expression; convenient application	Relatively low precision; limited estimation ability
Bilinear interpolation	Small standard deviation, high reliability of the model; high precision (highest precision among three methods)	A certain number of invalid data points can be generated; highly dependent on the learning and training samples; no direct and simple mathematical model; inconvenient practical application
Radial Basis Kernel Function Neural Network	Small standard deviation, high reliability of the model; relatively high precision	Error larger than bilinear interpolation; highly dependent on the learning and training samples; no direct and simple mathematical model; inconvenient practical application

3.2. Modeling Results of Motor Efficiency Based on the Novel Method Proposed and Analysis

According to Section 3.1, the results of modeling purely using PR have certain deficiencies with limited precision. Considering the process of the novel method proposed in Section 2.5, this paper chooses some new variables formed through the mapping transformation of the motor speed n_m and the motor torque T_m and then selects the variable with the maximum correlation coefficient through a correlation analysis. Table 7 shows the research results.

Table 7. Correlation coefficients of measured motor efficiency with multiple variables.

Variable	$\ln(n_m)$	$\ln(T_m)$	$\sin(n_m)$	$\sin(T_m)$	$\cos(n_m)$	$\cos(T_m)$	$\tan(n_m)$	$\tan(T_m)$	e^{T_m}
Correlation Coefficient	-0.184	0.836	0.027	-0.096	-0.049	0.087	0.028	0.008	0.019

Therefore, the research chooses $\ln(T_m)$, the variable with the maximum correlation, and introduces it into formula (13) and then forms the 10-parameter model for the efficiency of the motor used. The following is the model’s expression:

$$\eta_{m_novel} = a_0 + a_1 n_m + a_2 T_m + a_3 n_m T_m + a_4 n_m^2 + a_5 T_m^2 + a_6 T_m^3 + a_7 \ln(a_8 T_m + a_9) \quad (18)$$

Use the I-SA algorithm for parameter identification of the 10-parameter motor efficiency model. Figure 12 and Table 5 show the results of the 5-fold CV of 100 random tests.

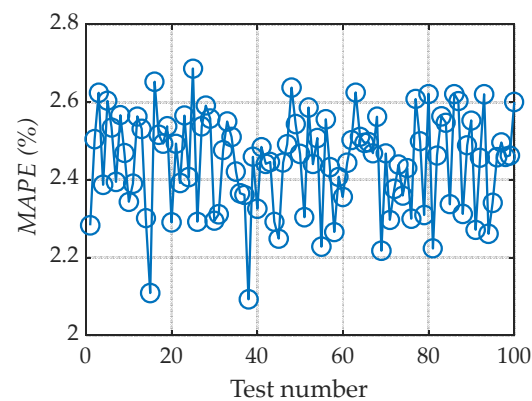


Figure 12. Results of 100 5-fold CV tests of novel method proposed. Note: *MAPE* is mean absolute percentage error.

According to Figure 12 and Table 5, the novel method proposed has high precision in motor efficiency modeling. The modeling result of the novel method improves greatly on the basis of PR. Additionally, the 5-fold CV results of 100 random tests (with a small standard deviation) show that the novel method has high reliability.

This paper uses the I-SA algorithm for the parameter identification of the novel model of a 5 kW motor and a 8 kW motor. Figure 13 shows iterative evolution curves.

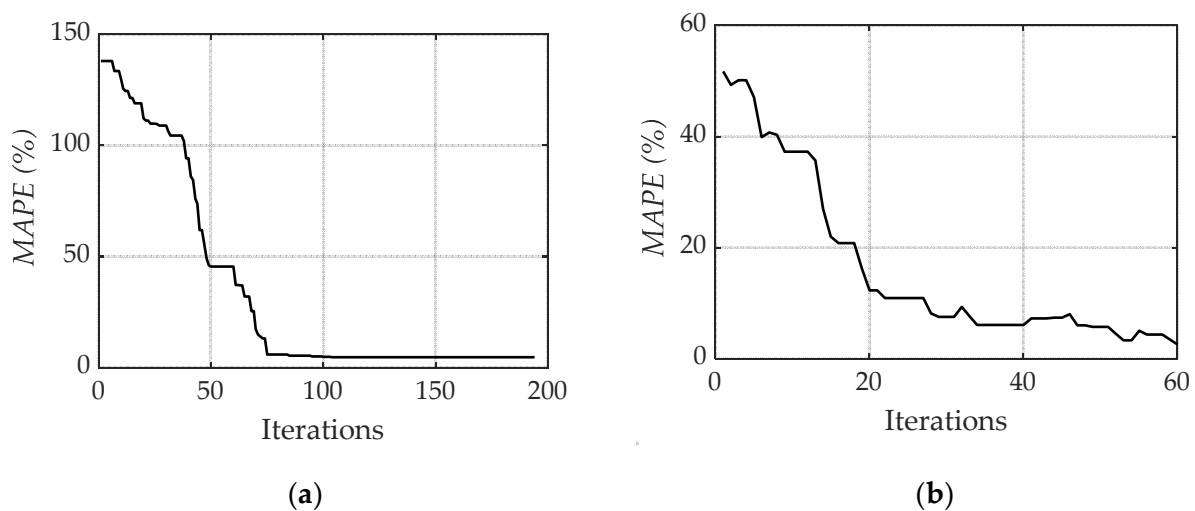


Figure 13. Iterative evolution curves of parameter identification of two motor efficiency models. (a) 8 kW motor; (b) 5 kW motor.

Figure 13 shows that the I-SA algorithm has a good application result for the parameter identification of the motor efficiency mode. The algorithm has a smaller number of iterations (declining to the ideal precision after about 60 iterations). In the implementing process of the algorithm, the value of an objective function is always declining, indicating that the I-SA avoids the problem of prematurity effectively.

Figure 14 shows the motor efficiency models in full working conditions.

Figure 14 shows that the motor efficiency models built with the novel method have ideal estimation results in the full working conditions of the motor speed n_m and the motor torque T_m . The MAPE of the 8 kW motor efficiency model's estimated value and all the test data is 4.768%, and the MAPE of the 5 kW motor efficiency model's estimated value and all the test data is 2.539%.

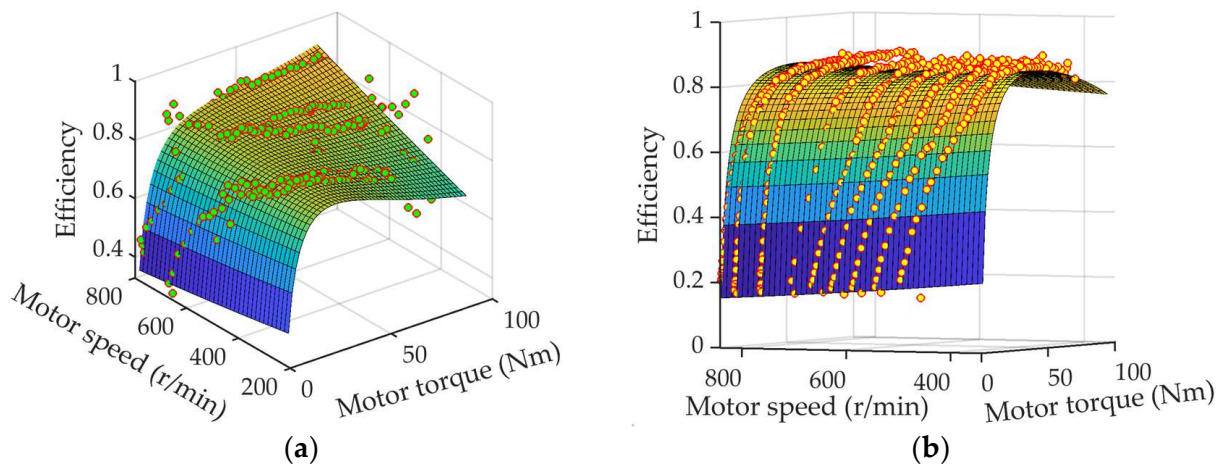


Figure 14. Efficiency models of two motors in full working conditions. (a) 8 kW motor; (b) 5 kW motor.

3.3. Comparison Results of Full Vehicle Efficiency Characteristics of Electric Tractors in Five Working Conditions and Analysis

Figure 15 shows the full vehicle working efficiency results of electric tractors of three different drive systems with different loads (showed as different reserve power) and running speeds (shown in the form of statistical histogram for the convenience of evaluation and analysis).

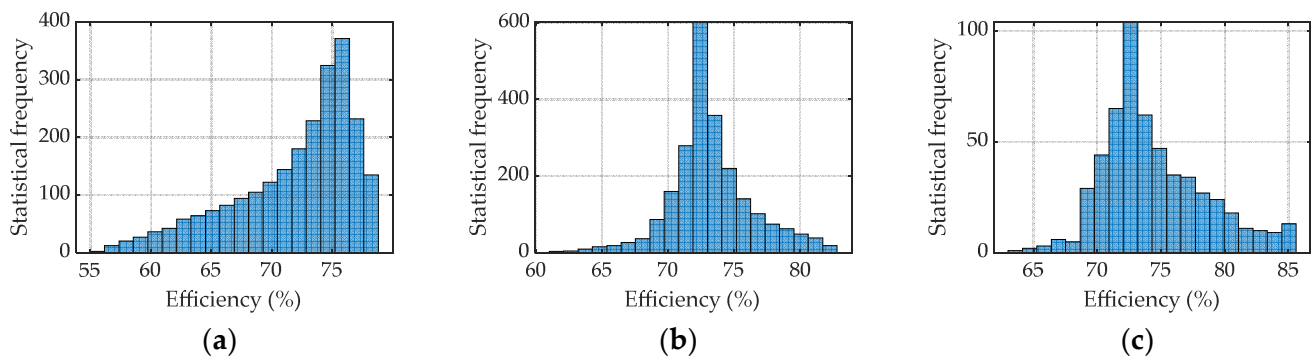


Figure 15. Estimation results of the full vehicle working efficiency of electric tractors with different drive systems. (a) 4 wheel independent drive system; (b) Rear wheel independent drive system; (c) Dual motor coupling drive system.

From Figure 15 we can see that the 4 wheel independent drive electric tractor's full vehicle efficiency shows the skewed distribution of which an efficiency lower than 70% accounts for 26.14%. The rear wheel independent drive electric tractor's efficiency distribution is nearly symmetric around the axis of 72%. The dual motor coupling drive electric tractor shows the slightly skewed distribution, but its distribution characteristic is opposite to that of the 4 wheel independent drive electric tractor, of which an efficiency higher than 75% accounts for 32.97%. Considering the range of the full working conditions selected, the dual motor coupling drive tractor shows better work efficiency as a whole.

Figure 16 shows the results of the normal road constant-speed running, transportation, ploughing, and rotary tillage working conditions. Table 8 gives the mean of the full vehicle efficiency of the electric tractors of three drive systems.

According to Figure 16 and Table 8, the dual motor coupling drive mode shows a relatively good full vehicle efficiency in most working conditions and has the highest average working efficiency with different loads and speeds. However, for the ploughing condition and the rotary tillage condition, the dual motor coupling drive electric tractor shows better efficiency characteristics. In the ploughing and rotary tillage conditions, the

performance of the efficiency characteristics of the three types of drives are not invariable, and each has its optimal working range.

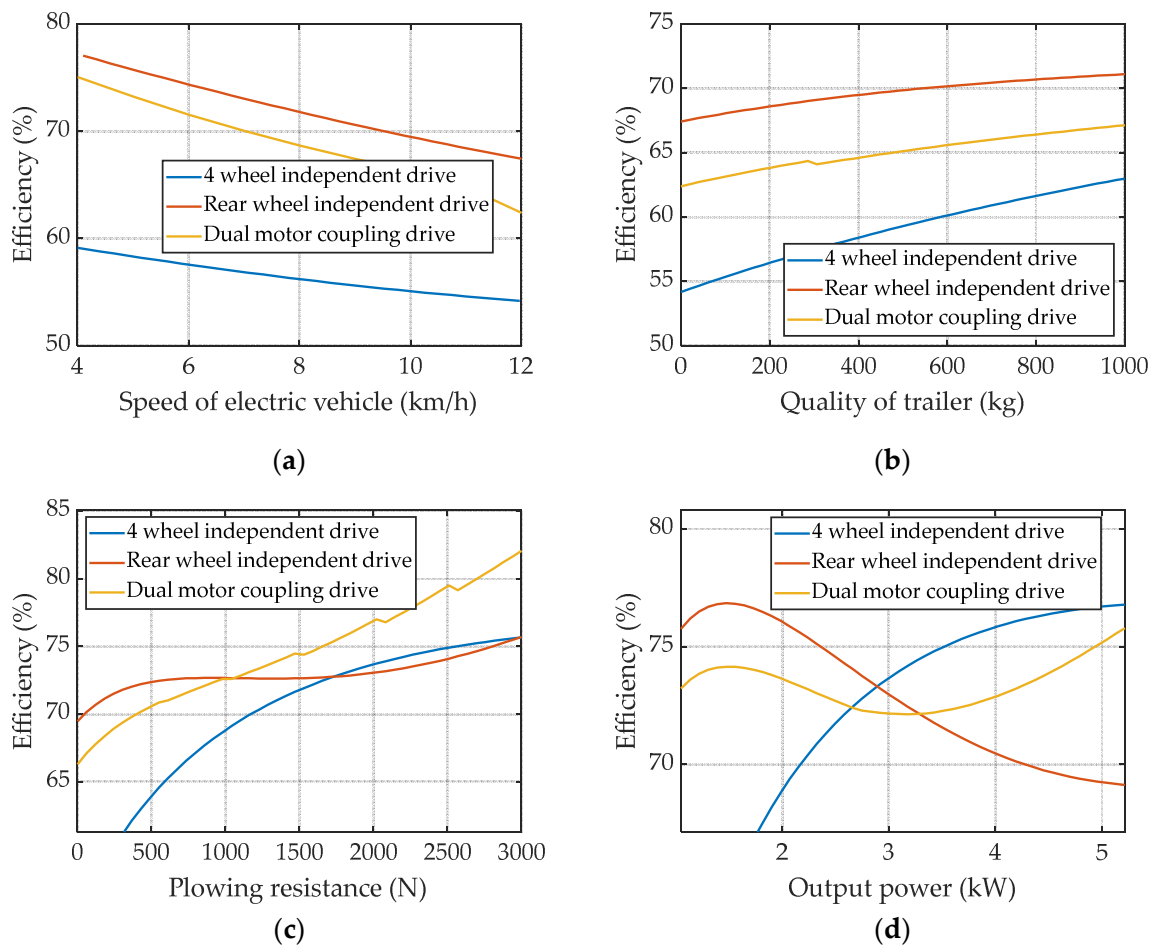


Figure 16. Estimation results of full vehicle efficiency of tractor in four working conditions. (a) Working condition of constant-speed running; (b) Working condition of transportation; (c) Working condition of ploughing; (d) Working condition of rotary tillage.

Table 8. Estimation results of mean of full vehicle efficiency of three drive systems for electric tractors.

Type of Drive	Mean of Electric Tractor Efficiency/%				
	Different Loads and Speeds	Constant-Speed Running	Transportation	Ploughing	Rotary Tillage
4 wheel independent	71.90	57.41	59.05	69.82	72.06
Rear wheel independent	73.26	71.86	69.65	72.96	72.86
Dual motor coupling	74.43	68.83	65.05	74.62	73.37

4. Conclusions

Compared with the three modeling methods (PR, BI, and RBF-NN), the proposed method in this paper not only has high model estimation precision (the mean of the MAPE of the 5-fold-CV of 100 random tests is 2.45 %, and the MAPE of all 853 measured data is 3.65 %) but also has high modeling reliability (the standard deviation of the MAPE of the 5-fold-CV of 100 random tests is 0.12 %). The structure of the new model proposed in this paper is relatively simple. Combined with a heuristic intelligent optimization algorithm, the model can be established only by identifying 10 unknown parameters. This is less dependent on the number of the test data. For the two motors used in this paper, the efficiency characteristics are highly correlated with the variables $\ln(T_m)$.

According to the various working conditions used in this study, this type of electric tractor equipped with a dual motor coupling drive system has the overall optimal economic performance (the highest full vehicle efficiency). From the analysis results of ploughing and rotary tillage conditions, the design of the electric tractor drive system should have the ability to switch between multiple driving modes (four wheel drive, rear wheel drive and coupling drive) to maximize the efficiency of the tractor under different working conditions.

Author Contributions: Methodology, Z.C.; software, Z.C. and H.Z.; validation, Z.C.; investigation, Z.C. and H.Z.; resources, Z.L. and H.Z.; writing—original draft preparation, Z.C.; writing—review and editing, Z.C. and Z.L.; supervision, Z.L.; project administration, Z.L. and Z.C. All authors have read and agreed to the published version of the manuscript.

Funding: This study was funded by the National Natural Science Foundation of China (grant number: 52105063), the National Key Research and Development Plan (2016YFD0701103), and the Metasequoia teacher research start-up fund of Nanjing Forestry University (163106061).

Institutional Review Board Statement: Not applicable.

Informed Consent Statement: Not applicable.

Data Availability Statement: The data presented in this study are available on demand from the corresponding author or first author at luzx@njau.edu.cn or chengzhun38@163.com.

Acknowledgments: The authors thank the National Natural Science Foundation of China (grant number: 52105063), the National Key Research and Development Plan (2016YFD0701103), and the Metasequoia teacher research start-up fund of Nanjing Forestry University (163106061) for funding. We also thank anonymous reviewers for providing critical comments and suggestions that improved the manuscript.

Conflicts of Interest: The authors declare no conflict of interest.

References

1. Tian, J.; Tong, J.; Luo, S. Differential steering control of four-wheel independent-drive electric vehicles. *Energies* **2018**, *11*, 2892. [[CrossRef](#)]
2. Tian, J.; Wang, Q.; Ding, J.; Wang, Y.Q.; Ma, Z.S. Integrated control with DYC and DSS for 4WID electric vehicles. *IEEE Access* **2019**, *7*, 124077–124086. [[CrossRef](#)]
3. Zhou, W.L.; Zheng, Y.P.; Pan, Z.J.; Lu, Q. Review on the Battery Model and SOC Estimation Method. *Processes* **2021**, *9*, 1685. [[CrossRef](#)]
4. Ren, G.Z.; Wang, J.Z.; Chen, C.L.; Wang, H.R. A variable-voltage ultra-capacitor/battery hybrid power source for extended range electric vehicle. *Energy* **2021**, *231*, 120837. [[CrossRef](#)]
5. Yu, Y.; Jiang, J.; Min, Z.; Wang, P.; Shen, W. Research on energy management strategies of extended-range electric vehicles based on driving characteristics. *World Electr. Veh. J.* **2020**, *11*, 54. [[CrossRef](#)]
6. Chang, C.C.; Zheng, Y.P.; Yu, Y. Estimation for battery state of charge based on temperature effect and fractional extended kalman filter. *Energies* **2020**, *13*, 5947. [[CrossRef](#)]
7. Nie, X.W.; Liu, Y.L.; Liu, Z.S. Parameter matching and transmission ratio optimization of pure electric car transmission system. *Mod. Manuf. Eng.* **2020**, *8*, 53–59.
8. Vijayagopal, R.; Rousseau, A. Electric truck economic feasibility analysis. *World Electr. Veh. J.* **2021**, *12*, 75. [[CrossRef](#)]
9. Zhao, Y.; Tatari, O. Carbon and energy footprints of refuse collection trucks: A hybrid life cycle evaluation. *Sustain. Prod. Consum.* **2017**, *12*, 180–192. [[CrossRef](#)]
10. Lee, D.Y.; Thomas, V.M.; Brown, M.A. Electric urban delivery trucks: Energy use, greenhouse gas emissions, and cost-effectiveness. *Environ. Sci. Technol.* **2013**, *47*, 8022–8030. [[CrossRef](#)]
11. Du, X.J.; Tian, Y.M.; Wang, Z.Y.; Wang, Y.Q.; Qiao, K.K. Simulation and optimization of aluminum frame electric car frontal collision. *J. Highw. Transp. Res. Dev.* **2017**, *34*, 136–142.
12. Vervaeke, M.; Calabrese, G. Prospective design in the automotive sector and the trajectory of the Bluecar project: An electric car sharing system. *Int. J. Veh. Des.* **2015**, *68*, 245–264. [[CrossRef](#)]
13. Petrovic, D.T.; Pesic, D.R.; Petrovic, M.M.; Mijailovic, R.M. Electric cars are they solution to reduce CO2 emission? *Therm. Sci.* **2020**, *24*, 2879–2889. [[CrossRef](#)]
14. Wang, W.W.; Gao, F.L.; Cheng, Y.T.; Lin, C. Multidisciplinary design optimization for front structure of an electric car body-in-white based on improved collaborative optimization method. *Int. J. Automot. Technol.* **2017**, *18*, 1007–1015. [[CrossRef](#)]

15. Moreda, G.P.; Munoz-Garcia, M.A.; Barreiro, P. High voltage electrification of tractor and agricultural machinery—A review. *Energy Convers. Manag.* **2016**, *115*, 117–131. [[CrossRef](#)]
16. Cheng, Z.; Lu, Z.X.; Qian, J. A new non-geometric transmission parameter optimization design method for HMCVT based on improved GA and maximum transmission efficiency. *Comput. Electron. Agric.* **2019**, *167*, 105034. [[CrossRef](#)]
17. Raikwara, S.; Tewaria, V.K.; Mukhopadhyay, S.; Verma, C.R.B.; Rao, M.S. Simulation of components of a power shuttle transmission system for an agricultural tractor. *Comput. Electron. Agric.* **2015**, *114*, 114–124. [[CrossRef](#)]
18. Fang, Q.R.; Shi, A.P.; Chen, A.Y.; Yin, S.Y. Research on driving torque control strategy of electric tractor. *J. Agric. Mech. Res.* **2021**, *43*, 243–248.
19. Chen, Y.N.; Xie, B.; Mao, E.R. Electric Tractor Motor Drive Control Based on FPGA. *IFAC Pap.* **2016**, *49*, 271–276. [[CrossRef](#)]
20. Gao, H.S.; Xue, J.L. Modeling and economic assessment of electric transformation of agricultural tractors fueled with diesel. *Sustain. Energy Technol. Assess.* **2020**, *39*, 100697. [[CrossRef](#)]
21. Li, T.H.; Xie, B.; Song, Z.H.; Li, J. Transmission characteristics of dual-motor coupling system for electric tractors. *Trans. Chin. Soc. Agric. Mach.* **2019**, *50*, 379–388.
22. Zhou, H.D.; Lu, Z.X.; Deng, X.T.; Zhang, C.; Luo, G.J.; Zhou, R.D. Study on torque distribution of traction operation of four wheel independent driven electric tractor. *J. Nanjing Agric. Univ.* **2018**, *41*, 962–970.
23. Han, B.; Liu, M.N.; Xu, L.Y. Analysis of steering characteristics of wheel-drive electric tractor. *J. Henan Univ. Sci. Technol. (Nat. Sci.)* **2021**, *42*, 38–45.
24. Xie, B.; Zhang, C.; Chen, S.; Mao, E.R.; Du, Y.F. Transmission performance of two-wheel drive electric tractor. *Trans. Chin. Soc. Agric. Mach.* **2015**, *46*, 8–13.
25. Li, S.Y.; Liu, M.N.; Xu, L.Y. Design and selection of power coupling device for electric tractor. *J. Mech. Transm.* **2021**, *45*, 75–82.
26. Ma, C.; Jin, S.W.; Yang, K.; Tan, D.; Gao, J.; Yan, D.C. Particle swarm optimization and real-road/driving-cycle analysis based powertrain system design for dual motor coupling electric vehicle. *World Electr. Veh. J.* **2020**, *11*, 69. [[CrossRef](#)]
27. Hu, J.J.; Zheng, L.L.; Jia, M.X.; Zhang, Y.; Pang, T. Optimization and model validation of operation control strategies for a novel dual-motor coupling-propulsion pure electric vehicle. *Energies* **2018**, *11*, 754. [[CrossRef](#)]
28. Li, T.H.; Xie, B.; Li, Z.; Li, J.K. Design and optimization of a dual-input coupling powertrain system: A case study for electric tractors. *Appl. Sci.* **2020**, *10*, 1608. [[CrossRef](#)]
29. Li, T.H.; Xie, B.; Wang, D.Q.; Zhang, S.L.; Wu, L.P. Real-time adaptive energy management strategy for dual-motor-driven electric tractors. *Trans. Chin. Soc. Agric. Mach.* **2020**, *51* (Suppl. S2), S530–S543.
30. Chen, Y.N.; Xie, B.; Du, Y.F.; Mao, E.R. Powertrain parameter matching and optimal design of dual-motor driven electric tractor. *Int. J. Agric. Biol. Eng.* **2019**, *12*, 33–41. [[CrossRef](#)]
31. Zhang, X.; Wang, S.T.; Zhang, X.; Wang, J. Torque coordination control strategy of in-wheel drive electric vehicle. *J. Beijing Jiaotong Univ.* **2017**, *41*, 121–129.
32. Hao, L.; Sun, B.H.; Li, G.; Guo, L.X. The eco-driving considering coordinated control strategy for the intelligent electric vehicles. *IEEE Access* **2021**, *9*, 10686–10698. [[CrossRef](#)]
33. Cheng, Z. I-SA algorithm based optimization design and mode-switching strategy for a novel 3-axis-simpson dual-motor coupling drive system of PEV. *World Electr. Veh. J.* **2021**, *12*, 221. [[CrossRef](#)]
34. Cheng, Z.; Lu, Z.X.; Dai, F. Research on HMCVT Efficiency Model Based on the Improved SA Algorithm. *Math. Probl. Eng.* **2019**, *2019*, 2856908. [[CrossRef](#)]
35. Jiao, W.M.; Ma, F.; Yang, Y.D.; Zhao, X.X. Calculation of transmission ratio and efficiency of planetary gear box. *J. Mech. Transm.* **2012**, *36*, 114–116.
36. Zhou, H.D. *Research on Torque Distribution Strategy of Four-Wheel Independent Drive Electric Tractor*; Nanjing Agricultural University: Nanjing, China, 2018.
37. Qian, Y.; Cheng, Z.; Lu, Z.X. Bench testing and modeling analysis of optimum shifting point of HMCVT. *Complexity* **2021**, *2021*, 6629561. [[CrossRef](#)]
38. Ji, X.Y.; Hao, H.M.; Yang, K.; Wang, H.; Li, B.; Huang, J.H. Dead-zone compensation for proportional directional valve based on bilinear interpolation control strategy. *Chin. Hydraul. Pneum.* **2021**, *45*, 56–62.
39. Khan, S.; Naseem, I.; Malik, M.A.; Togneri, R.; Bennamoun, M. A fractional gradient descent-based RBF neural network. *Circuits Syst. Signal Processing* **2018**, *37*, 5311–5332. [[CrossRef](#)]
40. Khan, S.; Naseem, I.; Togneri, R.; Bennamoun, M. A novel adaptive kernel for the RBF neural networks. *Circuits Syst. Signal Processing* **2017**, *36*, 1639–1653. [[CrossRef](#)]
41. Kilic, E.; Ozcalik, H.R.; Sit, S. Adaptive controller with RBF neural network for induction motor drive. *Int. J. Numer. Model. Electron. Netw. Devices Fields* **2018**, *31*, e2280. [[CrossRef](#)]
42. Cheng, Z.; Lu, Z.X. A novel efficient feature dimensionality reduction method and its application in engineering. *Complexity* **2018**, *2018*, 2879640. [[CrossRef](#)]
43. Xu, X.M.; Lin, P. Parameter identification of sound absorption model of porous materials based on modified particle swarm optimization algorithm. *PLoS ONE* **2021**, *16*, e0250950. [[CrossRef](#)] [[PubMed](#)]
44. Wang, H.; Zheng, Y.P.; Yu, Y. Joint estimation of soc of lithium battery based on dual kalman filter. *Processes* **2021**, *9*, 1412. [[CrossRef](#)]

45. Li, Y.J.; Ma, Z.S.; Zheng, M.; Li, D.X.; Lu, Z.H.; Xu, B. Performance analysis and optimization of a high-temperature PEMFC vehicle based on particle swarm optimization algorithm. *Membranes* **2021**, *11*, 691. [[CrossRef](#)] [[PubMed](#)]
46. Cheng, Z.; Lu, Z.X. Research on the PID control of the ESP system of tractor based on improved AFSA and improved SA. *Comput. Electron. Agric.* **2018**, *148*, 142–147. [[CrossRef](#)]
47. Cheng, Z.; Lu, Z.X. Semi-empirical model for elastic tyre trafficability and methods for the rapid determination of its related parameters. *Biosyst. Eng.* **2018**, *174*, 204–218. [[CrossRef](#)]
48. Wang, G. *Study on Characteristics, Control and Fault Diagnosis of Tractor Hydro-Mechanical CVT*; Nanjing Agricultural University: Nanjing, China, 2014.